Development of a Mathematical Model for Studying Bioethanol–Water Separation Using Hydrophilic Polyetherimide Membrane

M. E. T. Alvarez, E. B. Moraes, W. A. Araujo, R. Maciel Filho, M. R. Wolf-Maciel

School of Chemical Engineering, Separation Process Development Laboratory, State University of Campinas, UNICAMP, 13083-970, Campinas-SP, Brazil

ABSTRACT: An essentially predictive mathematical model was developed to simulate pervaporation process. The group contribution method UNIFAC was used for calculating the upstream activity coefficients. The diffusion coefficient in the membrane was predicted using free-volume theory. Free-volume parameters were determined with viscosity and temperature data, and the binary interaction solvent–polymer parameter was calculated by a group-contribution lattice-fluid equation of state (GCLF-EOS). A simulator named PERVAP was developed applying the mathematical model. Pervaporation process was simulated for separating bioethanol–water through poly-etherimide membrane. The simulated results were validated using experimental data of bioethanol/water separation through polyetherimide membrane. The model presented a satisfactory performance compared to experimental data. Related to the simulation of the studied separation, a 99% molar enriched bioethanol stream was obtained with a recovery of 94%. © 2007 Wiley Periodicals, Inc. J Appl Polym Sci 107: 2256–2265, 2008

Key words: pervaporation; solution–diffusion mechanism; free volume theory; bioethanol–water mixture; polyetherimide membrane

INTRODUCTION

Pervaporation, a term derived from two major operations involved in the separation process, namely, permeation and evaporation, is defined as a separation process in which a liquid feed mixture is separated by means of selective diffusion-vaporization through a nonporous membrane.[1] This is potentially an effective process for separating azeotropic mixtures with components of low molecular weight. The solution–diffusion mechanism is adopted to describe pervaporative transport through dense membranes and this has become the accepted pattern for this process. According to this mechanism, the transport occurs in three steps: (a) selective sorption of the components on the membrane surface; (b) diffusion of the components through the membrane; (c) desorption on the permeate side.[2] Pervaporation-based process holds a large potential for utilization by the traditional chemical industry and by emerging areas such as environmental and biochemical engineering, using dense membranes to separate different types of mixtures and it represents an alternative unit operation for replacing conventional separation processes usually applied to remove volatile organic compounds from water,[1] and for recovering key aroma compounds.[2] From the stand point of performance, this membrane technology is considered as a reliable separation process compared to conventional processes. Energy savings, safety, and environmentally sustainable feature are among the advantages of pervaporation, when it is used for separating organic–organic mixtures. These issues support the feasibility of this process.[3]

Several studies were already carried out to describe and understand the mass transfer through the membrane in this process, and mathematical models were proposed taking into account the effects of the variables on the process performance.[4–9] Recently, Hoda et al.[10] developed a model combining solution–diffusion theory with mass, momentum, and energy balances considering a hollow fiber module, and Peng et al.[11] presented a predictive model for permeate flux determination based on solubility prediction of components in the membrane by UNIFAC-FV (UNIquac Functional-group Activity Coefficient-Free-Volume) and diffusion coefficient calculation by free-volume theory,[12,13] and satisfactory results were obtained when compared with experimental data. However, this model underestimate selectivity factor when low temperatures were investigated. Bearing all these points in mind, the

objective of this work is the development of a detailed mechanistic model to investigate how the design and operation parameters influence the overall process performance. The proposed mathematical model is based on the solution–diffusion mechanism for separating binary mixtures by pervaporation process. A predictive approach was considered to determine the model parameters. The development of the PERVAP software based on the proposed model was carried out in this work. The simulation results were validated with experimental data,[14] and the pervaporation performance for separating the mixture bioethanol–water through a hydrophilic membrane was investigated.

PERVAPORATION MODEL

The model approach that seems to better represent the mass transfer phenomena of the components through the membrane is that based on the solution–diffusion mechanism. The mass transfer of the permeate components through the membrane is presented in Figure 1.

The following steps describe the permeation profile based on the solution diffusion mechanism:

1. Solution of the components through the feed/membrane interface;
2. Diffusion of the components through the membrane;
3. Desorption of the components of the permeate side.

Assuming that the system is in equilibrium in both sides of the membrane interface (upstream and downstream), the expressions of the permeate flux can be obtained from the mass transport in the boundary layer (upstream) and in the membrane.

Transport in the boundary layer

Considering Figure 1, at steady state, according to the first Fick's law, the molar flux in the boundary layer, δ_{bl}, for component i, can be expressed as shown in Ref. 4:

$$J_i = \frac{D_{i,F} Pe}{\delta_{bl}} \left(\frac{C_{i,F} \exp(Pe) - C_{i,F}^m}{\exp(Pe) - 1} \right) \qquad (1)$$

where Pe is the Peclet number; $D_{i,F}$ is the diffusion coefficient of component i in the liquid feed, which can be estimated by Wilke and Chang equation:[15]

$$D_{i,F} = \frac{7.4 \times 10^{-8} (\phi M_j)^{1/2} T}{\mu_j (v_i)^{0.6}} \qquad (2)$$

According to Gref,[16] the convective flux can be ignored if the membrane presents a high selectivity to a component or the feed side operates in a turbulent regime. Thus, the Peclet number is equivalent to $Pe \ll 1$. Considering that the system operates in a regime of $Pe \ll 1$, eq. (1) can be reduced to a simpler expression:[4]

$$J_i = \frac{D_{i,F}}{\delta_{bl}} \left(C_{i,F} - C_{i,F}^m \right) \qquad (3)$$

where the concentration of component i in the feed phase $(C_{i,F})$ and in the membrane $(C_{i,F}^m)$ can be solved expressing the driving force in terms of activities.

Equilibrium in the feed interface

The feed-phase composition can be determined from the chemical potential at the feed membrane interface.[17] By definition, the chemical potential in the boundary region of the feed phase as well as of the membrane are expressed by the following equation:

$$\mu_{i,F} = \mu_{i,0} + RT \ln a_{i,F} + \int_{P_P}^{P_F} v_{i,F} \, dP \qquad (4)$$

$$\mu_{i,F}^m = \mu_{i,0} + RT \ln a_{i,F}^m + \int_{P_P}^{P_F^m} v_{i,F}^m \, dP \qquad (5)$$

where $v_{i,F}$ is the molar partial volume of component i in the feed phase, v_i^m is the molar partial volume of component i in the membrane, which are assumed to be constant. Because in the pervaporation process the feed is in the liquid phase, it is assumed that the molar partial volume of the permeant compound in the membrane is equal to the feed molar partial volume. In the equilibrium, the permeant concentration in the membrane interface can be calculated by thermodynamic equations. Assuming that the membrane is in contact with the feed phase and that the chemical potential in the membrane interface and in the feed solution is the same, then:

$$\mu_{i,F} = \mu_{i,F}^m \qquad (6)$$

Thus, the chemical potential can be expressed on the basis of the activity. Considering the activity equal to the product of concentration and the activity coefficient, the concentration in the membrane interface of components i and j can be related with the concentration of the feed phase. If the molar volume is constant in the feed with an equal value in the membrane, and whether feed pressure is larger than the permeate pressure, eqs. (4) and (5) can be applied in eq. (6) thus:
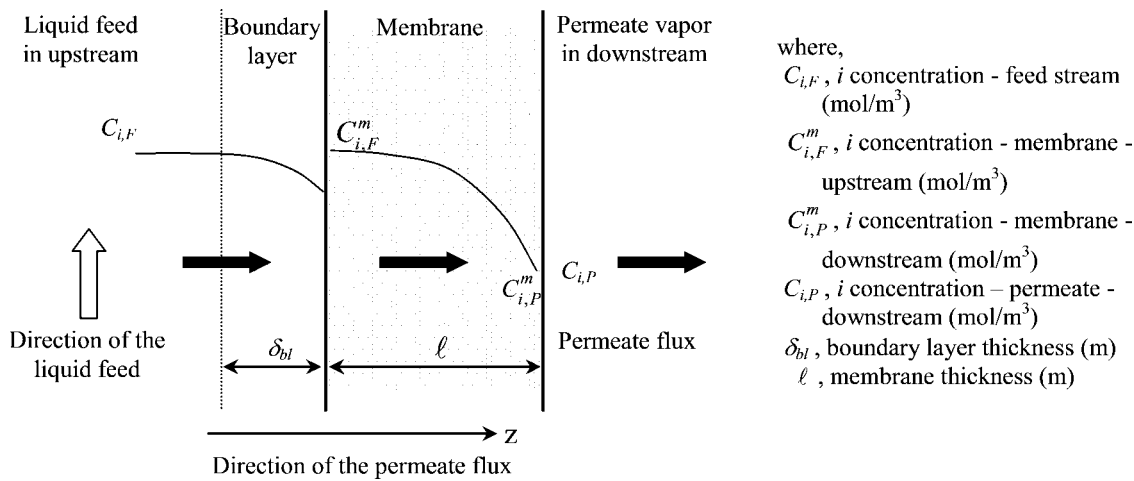
Figure 1 Concentration profile of the compound i through the membrane.

where,

$C_{i,F}$, i concentration - feed stream (mol/m^3)

$C_{i,F}^m$, i concentration - membrane - upstream (mol/m^3)

$C_{i,P}^m$, i concentration - membrane - downstream (mol/m^3)

$C_{i,P}$, i concentration – permeate - downstream (mol/m^3)

δ_{bl}, boundary layer thickness (m)

ℓ , membrane thickness (m)

$$\overline{\gamma}_i^m C_{i,F}^m = \gamma_{i,F} x_{i,F} \exp\left[\frac{v_{i,F}}{RT}(P_F - P_F^m)\right] \qquad (7)$$

On the other hand, if the membrane pressure at interface is equal to the upstream pressure, after solving the above-exponential expression, the results obtained is equal to one, thus:[6,7]

$$\gamma_{i,F} x_{i,F} = \overline{\gamma}_i^m C_{i,F}^m \qquad (8)$$

$$\gamma_{j,F} x_{j,F} = \overline{\gamma}_j^m C_{j,F}^m \qquad (9)$$

where $C_{i,F}^m$ and $C_{j,F}^m$ are the molar concentrations in the membrane interface of the components i and j respectively, which can be determined from experimental solubility data of components in the membrane.[6,7] The activity coefficient of component i in the feed ($\gamma_{i,F}$) is determined through the UNIFAC method. Thus, the activity coefficients in the membrane for components i ($\overline{\gamma}_i^m$) and j ($\overline{\gamma}_j^m$) can be calculated from eqs. (8) and (9).

Transport in the membrane

At steady state, the diffusive flux of each component, considering the interfaces of the membrane with the feed phase and the permeate phase, is defined as:

$$J_i = \frac{D_i^m}{\ell}\left(C_{i,F}^m - C_{i,P}^m\right) \qquad (10)$$

where D_i^m is the diffusivity coefficient of component i in the membrane. Solving eqs. (3) and (10), it gives

$$J_i = \frac{\frac{D_i^m}{\ell} \times \frac{D_{i,F}}{\delta_{bl}}}{\frac{D_i^m}{\ell} + \frac{D_{i,F}}{\delta_{bl}}}\left(C_{i,F} - C_{i,P}^m\right) \qquad (11)$$

In the permeation process, the permeants follow a concentration profile through the membrane, from

the upstream up to the downstream. So, the concentration of permeants i and j in the membrane in the downstream (permeate phase) is determined considering equilibrium in the permeate side.

Equilibrium in the permeate interface

The chemical potentials in the permeate membrane interface are expressed by

$$\mu_{i,P} = \mu_{i,0} + RT \ln a_{i,P} + \int_{P_F}^{P_P} v_{i,P}\, dP \qquad (12)$$

$$\mu_{i,P}^m = \mu_{i,0} + RT \ln a_{i,P}^m + \int_{P_P^m}^{P_P} v_{i,P}^m\, dP \qquad (13)$$

Assuming that the system is in equilibrium, the chemical potentials in the membrane interface and in the permeate one are equals. So, simplifying:

$$a_{i,P}^m = a_{i,P} \exp\left[-\frac{v_i(P_F - P_P)}{RT}\right] \qquad (14)$$

$$\overline{\gamma}_i^m C_{i,P}^m = \frac{P_P Y_{i,P}}{P_i^{sat}} \exp\left[-\frac{v_i(P_F - P_P)}{RT}\right] \qquad (15)$$

If the membrane pressure is assumed to be equal to the feed-phase pressure, and that the membrane pressure is higher than the permeate-phase pressure, then the exponential term is equal to one,[18] so

$$\overline{\gamma}_i^m C_{i,P}^m = \frac{P_P y_{i,P}}{P_i^{sat}} \qquad (16)$$

$$\overline{\gamma}_j^m C_{j,P}^m = \frac{P_P y_{j,P}}{P_j^{sat}} \qquad (17)$$

The selectivity for the pervaporation process is defined by the following equation:

$$\alpha = \frac{y_{i,p}/y_{j,p}}{x_{i,F}/x_{j,F}} \tag{18}$$

The compositions $y_{i,P}$ and $y_{j,P}$ are calculated using the Eq. (18), expressed by:

$$y_{i,p} = \frac{x_{i,F}\,\alpha}{1 + (\alpha - 1)x_{i,F}} \tag{19}$$

$$y_{i,p} = \frac{1 - x_{i,F}}{1 + (\alpha - 1)x_{i,F}} \tag{20}$$

The concentration in the membrane (permeate phase), according to Brun et al.,[6] can be expressed substituting eqs. (19) and (20) into eqs. (16) and (17), respectively, so that the following equations can be written as

$$C_{i,P}^m = \frac{x_{i,F}\,\alpha\,p}{\overline{\gamma}_i^m \left[1 + (\alpha - 1)x_{i,F}\right]} \tag{21}$$

$$C_{j,P}^m = \frac{(1 - x_{i,F}\,p)P_i^{sat}}{\overline{\gamma}_j^m \left[1 + (\alpha - 1)x_{i,F}\right] P_j^{sat}} \tag{22}$$

where $p = P_P\,P_i^{sat}$ is the partial pressure, P_P is the downstream pressure (kPa), P_i^{sat} is the vapor pressure (kPa) of component i, α is the selectivity, $x_{i,F}$ is the feed mole fraction of component i, and $\overline{\gamma}_i^m$ and $\overline{\gamma}_j^m$ are the activity coefficients in the membrane for components i and j, respectively.

Substituting eq. (21) into eq. (11), it gives

$$J_i = \frac{D_i^m D_{i,F}}{(D_i^m \delta_{bl} + D_{i,F}\,\ell)\,\overline{\gamma}_i^m} \left(x_{i,F}\gamma_{i,F} - \frac{x_{i,F}\,\alpha\,p}{1 + (\alpha - 1)x_{i,F}} \right) \tag{23}$$

The same procedure was applied for component j.

Considering that the mass transfer in the feed phase does not present resistance over the boundary layer, it can be assumed that the boundary layer thickness, δ_{bl}, can be negligible. So, eq. (23) is reduced to

$$J_i = \frac{D_i^m}{\ell\,\overline{\gamma}_i^m} \left(x_{i,F}\,\gamma_{i,F} - \frac{x_{i,F}\,\alpha\,p}{1 + (\alpha - 1)x_{i,F}} \right) \tag{24}$$

where the diffusion coefficient of component i in the membrane, D_i^m in this work, was predicted by the free-volume theory.

Prediction of the diffusion coefficient

Vrentas and Duda[12,13] proposed an equation for the prediction of the diffusion coefficient based on the free-volume theory. The diffusion coefficient of the solvent (component i) in the membrane, D_i^m, can be predicted by the following equation:

$$D_i^m = D_0(1 - \phi_1)^2(1 - 2\chi\phi_1)\exp\left(\frac{-E}{RT}\right)$$

$$\times \exp\left(-\frac{\omega_1\widehat{V}_1^* + \xi\omega_2\widehat{V}_2^*}{\frac{K_{11}}{\gamma}\omega_1(K_{21} - T_{g1} + T) + \frac{K_{12}}{\gamma}\omega_2(K_{22} - T_{g2+T})} \right) \tag{25}$$

where D_0 is a constant pre-exponential factor, E is the energy required to overcome attractive forces from neighboring molecules, γ is an overlap factor for free-volume, $\widehat{V}_1^*$ and $\widehat{V}_2^*$ are the specific critical hole free volumes of component i and the polymer required for jump, ω_1 is the solvent weight fraction, ω_2 is the polymer weight fraction, ξ is the ratio of critical molar volume of solvent jumping unit to that of polymer jumping unit, K_{11} and K_{21} are the solvent free-volume parameters, K_{12} and K_{22} are polymer free-volume parameters, ϕ_1 is the component volume fraction, χ is the component/polymer interaction parameter, which was predicted in this work by the group contribution method,[19] T_{gi} is the solvent glass transition temperature, and T is the temperature and R is the gas constant.

From eq. (24), 10 parameters need to be known. The free-volume parameters of the solvent and of the polymer are calculated from viscosity data and temperature. Hong[20] showed the parameters determined for some components and polymers.

The results of the energy, E, for different components, were studied by Hong.[20] It was observed that, when the component mass fraction is around 1.0, the E values are relatively low when compared with the values determined by diffusion experiments and that the E values do not vary among the different components studied. Therefore, assumption that $E = 0$ was already evaluated, and it was not observed influence on the values of diffusion coefficient. This can be validated when the diffusion values were compared with experimental data. So, in this work, the Hong approach was considered and E values for bioethanol, and water were assumed as being equal to zero.

Calculation of the binary interaction parameter of solvent–polymer

The interaction parameter between the solvent and the polymer can be determined using the Flory-Huggins theory[21] from solubility data, in which the volume fraction between the solvent and the polymer in the equilibrium is known as a function of the solvent vapor pressure. However, High and Danner[22] have developed new group contribution lattice-fluid equation of state to predict the equilibrium
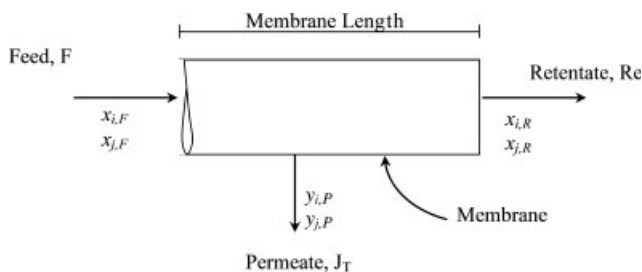
Figure 2 Scheme of the feed, permeate, and retentate flow rates in a tubular pervaporation membrane.

properties of polymer–solvent solutions. Lee and Danner[19] have made a modification of this equation to improve the capacity to predict the equilibrium properties and the binary interaction parameter, δ_{12}, between solvent and polymer. Therefore, to obtain an accurate predictive model, an equation was developed from the group contribution method, considering the binary interaction parameter as constant and independent of the temperature and of the concentration. This parameter can be calculated from binary group parameters between the groups m and n and from binary interaction parameters of the group α_{mn}, expressed by the following equation:

$$\delta_{12} = \chi = \sum_m \sum_n \Theta_m^{(M)} \Theta_n^{(M)} \alpha_{mn} \qquad (26)$$

where $\Theta_m^{(M)}$ is the superficial area fraction of the group m in the mixture and is given by:

$$\Theta_m^{(M)} = \frac{\sum_i n_m^{(i)} Q_m}{\sum_k \sum_i n_k^{(i)} Q_k} \qquad (27)$$

where $n_m^{(i)}$ is the number of groups m in component i, and Q_m is the surface area parameter of group m.

The values of the UNIFAC surface area parameters were calculated by Fredenslund et al.[23,24] The binary interaction parameter of the groups, α_{mn}, were calculated and tabled by Lee and Danner.[19]

Selectivity determination

The selectivity, for the pervaporation process, can be obtained from flux equations for the components i and j, which is expressed by eq. (28):

$$\alpha_{i,j} = \frac{D_i^m \overline{\gamma}_j^m \left(\gamma_{i,F} x_{i,F} - \frac{x_{i,F} \alpha p}{1+(\alpha-1)x_{i,F}} \right)(1 - x_{i,F})}{D_j^m \overline{\gamma}_i^m \left(\gamma_{j,F} x_{j,F} - \frac{(1-x_{i,F})p\,P_i^{sat}}{P_j^{sat}[1+(\alpha-1)x_{i,F}]} \right) x_{i,F}} \qquad (28)$$

Determination of permeate composition

The composition of component i in downstream, $y_{i,P}$, can be determined considering the permeate total

flux, which is the sum of the permeate component partial fluxes, that is, $J_T = J_i + J_j$, as presented in eq. (29):

$$y_{i,P} = \frac{J_i}{J_i + J_j} \qquad (29)$$

Using the equations described in this model, the PERVAP simulator was developed to represent the pervaporation process.

Mass balance and recovery in the pervaporation process

In this study, the scheme presented in Figure 2 was used to determine compositions and fluxes for feed and retentate streams. A tubular module is considered for separating the binary mixture.[25]

Related to pervaporator mass balance, the equations to calculate the retentate flux and composition are, respectively:

$$Re = \frac{J_T A (y_{j,P} - x_{j,F})}{x_{j,F} - x_{j,R}} \qquad (30)$$

$$x_{i,R} = \frac{F(x_{i,F}) - J_T A(y_{i,P})}{Re} \qquad (31)$$

The recovery of the process is defined by

$$Recovery = \frac{Re(1 - x_{j,R})}{F(1 - x_{j,F})} \qquad (32)$$

METHODS

In this study, the separation of the mixture bioethanol/water through polyetherimide (PEI) membranes was simulated assuming a tubular module with one-square meter of area. Thus, purity and recovery were evaluated on this design basis. The effect of the process variables and the validation of the proposed model were evaluated using a FORTRAN software named ''PERVAP.'' Experimental data from literature were used in the validation step.[14] The commercial PEI membrane (Ultem-1000, General Electric) was used.[14] The operating conditions considered for simulation were operating temperature: 310.15 K; downstream pressure (permeate): 0.133 kPa, and membrane thickness: 160 μm. The repetitive unit of the polimeric chain of PEI is represented in Figure 3.
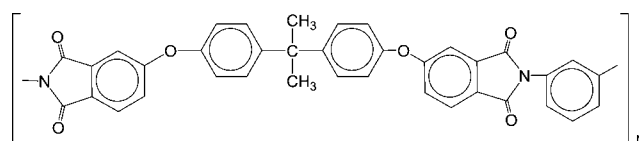
Figure 3 Polyetherimide, ULTEM-1000.

RESULTS AND DISCUSSION

Considering the polimeric structure of the PEI membrane, the specific critical hole free volume was estimated by the group contribution method[26] and the binary interaction parameter was estimated by the group contribution method of Lee and Danner,[19] considering the molecular groups. The polymer free-volume parameters were calculated from viscosity and temperature of the pure polymer data as described by Hong.[20] The experimental data of viscosity and temperature are from the literature.[27] Table I presents the free-volume parameters estimated for the PEI membrane, and Table II presents the free-volume parameters for bioethanol and water obtained using the methods described by Hong,[20] the binary interaction parameters of polymer/solvent, and the ratio of critical molar volume of solvent jumping unit to that of polymer jumping unit, ξ.

Considering the data described in these tables, the parameters are introduced in the diffusivity equation [eq. (24)], and the diffusion coefficients of the components in the membrane were calculated. In this work, the diffusion coefficient in the membrane for the individual components is determined considering infinite dilution[28] and assuming that it does not depend on the concentration. The activity coefficients of the feed components in the permeation equation for bioethanol and water are estimated by the group contribution method UNIFAC and the vapor pressure by the Antoine equation. The activity coefficients in the membrane, $\overline{\gamma}_i^m$ and $\overline{\gamma}_j^m$, were estimated from experimental data of flux and composition. It is important to mention that the values of $\overline{\gamma}^m$ are values calculated from eqs. (7) and (8), which can be obtained from experimental data of sorption, as described by Brun et al.[7] Table III presents the calculated data of the activity and diffusion coefficients in the membrane.

The data presented in Tables I–III were inputs to the PERVAP simulator to carry out the simulation of the pervaporation process.

According to Figure 4, it is observed that the bioethanol flux in the permeate side increases increasing the feed bioethanol mole fraction, whereas the water flux decreases. However, the bioethanol flux is higher than the water for bioethanol mole fractions above 0.95. On the other hand, the results obtained with the model proposed in this study fitted satisfactorily to the experimental data.[14] This scenario encourages the application of PERVAP simulator for other systems.

Figure 5 illustrates the behavior of the selectivity in function of the bioethanol mole fraction in the feed. It can be observed that for low concentration of bioethanol in the feed and consequently, high concentration of water, the selectivity is also low. This occurs because the separation of water becomes more difficult. On the other hand, when the bioethanol mole fraction is higher than 0.6, the selectivity increases, indicating a better water separation through the membrane. Thus, preferentially, for higher bioethanol mole fraction in the feed as, for example, above 0.90 mol of bioethanol at 101.33 kPa, around the azeotropic point, the separation is quite good, becoming an attractive application for this azeotropic system. The selectivity data calculated with the proposed model show good agreement with the experimental data.[19]

The PEI membrane, as already mentioned, is characterized by presenting a higher water affinity, being recommended preferentially for high concentrations of bioethanol in the feed. Figure 6 illustrates the variation of the bioethanol mole fraction in the permeate side with the bioethanol mole fraction in the feed. It is observed that the bioethanol mole fraction in permeate is always lower than the bioethanol mole fraction in the feed, indicating that water is always the component preferentially separated through the membrane, independently of the bioethanol mole fraction in the feed. Also, this figure shows that the azeotropic point was eliminated. Again, it is possible to see that the experimental results fit quite well with the calculated values.

Concerning dehydration of water–organic mixtures through pervaporation, the pressure of the permeate side (downstream pressure) is one of the

TABLE II
Free-Volume Parameters Estimated and Predicted for Bioethanol and Water

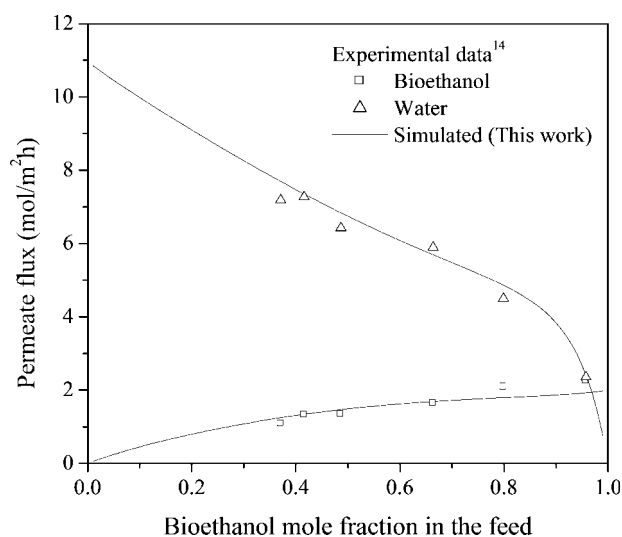| Components	$\widehat{V}_1^*$	K_{11}/γ	$K_{21} - T_{g1}$	D_o	χ	ξ	E
Bioethanol	0.985	0.312×10^{-3}	111.80	11.60×10^{-4}	0.043	0.124	0
Water	1.071	2.180×10^{-3}	-152.29	8.55×10^{-4}	0.053	0.035	0

Data applied to predict the diffusion coefficient.

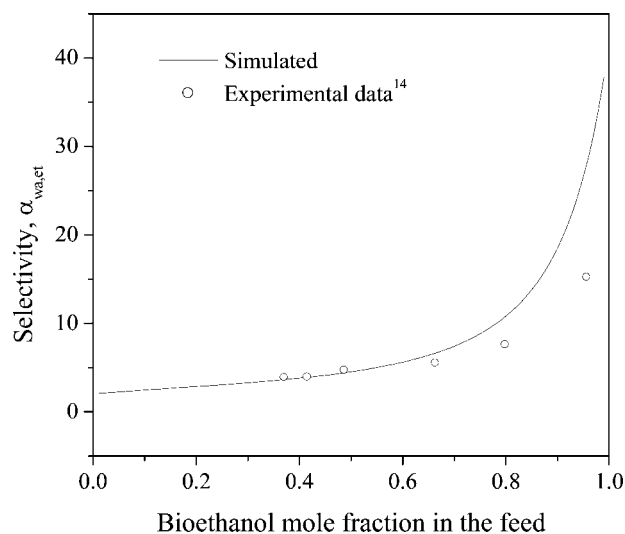**TABLE III**
Activity and Diffusion Coefficients in the Membrane

Components	$\overline{\gamma}_i^m$	$\overline{\gamma}_j^m$	D_i^m	D_j^m
Bioethanol (i) and water (j)	2.670	0.211	8.62×10^{-4}	3.78×10^{-4}

important variables to be controlled, because it influences on the enrichment and concentration of the organic component, in this case, bioethanol. In Figure 7, it can be observed that for higher permeate pressure, lower is the permeate flux, for a bioethanol mole fraction in the feed of 0.415. For a hydrophilic membrane, the water flux in the permeate is always higher than the bioethanol flux. However, the ratio of the bioethanol flux by the water flux presents a decrease of 0.18 (at 0.133 kPa) to 0.17 (at 4.5 kPa), what indicates a small reduction of the bioethanol flux in relation to the water flux, increasing the pressure. This causes an increase in the selectivity, what can be proven when the behavior of the selectivity with the pressure is analyzed, as presented in Figure 8, in which low pressures in the permeate indicate low selectivity.

The impact of feed bioethanol mole fraction in the permeate flux was evaluated. Figure 9 illustrates a decrease of the permeate flux increasing the pressure. For pressures equal to 3 and 4 kPa, it is observed an increase of the fluxes until reaching a maximum and, after, they decrease. This scenario indicates a higher diffusion of the components through the membrane with the increase of bioethanol mole fraction. For bioethanol mole fractions higher than 0.6, the total flux for the studied pressures tends to decrease and to converge to the same


Figure 5 Variation of the selectivity in function of the bioethanol mole fraction in the feed ($P_2 = 0.133$ kPa, $T = 310.15$ K).

point. This indicates that the permeate pressure does not have a significant impact on the separation of the concentrated mixtures in bioethanol.

Retentate purity and recovery evaluation

It was evaluated that the bioethanol purity in the retentate, the possibility of dehydration of an azeotropic mixture of bioethanol/water through the pervaporation process, which contains $\sim 89.0\%$ (mol) of bioethanol at 101.33 kPa was studied. Residual water content in the retentate lower than 6.0% (mol) was assumed. Figure 10 illustrates the potential of the pervaporation for separating the azeotropic mixture

Figure 4 Variation of the permeate flux in function of the feed bioethanol mole fraction ($P_2 = 0.133$ kPa, $T = 310.15$ K).
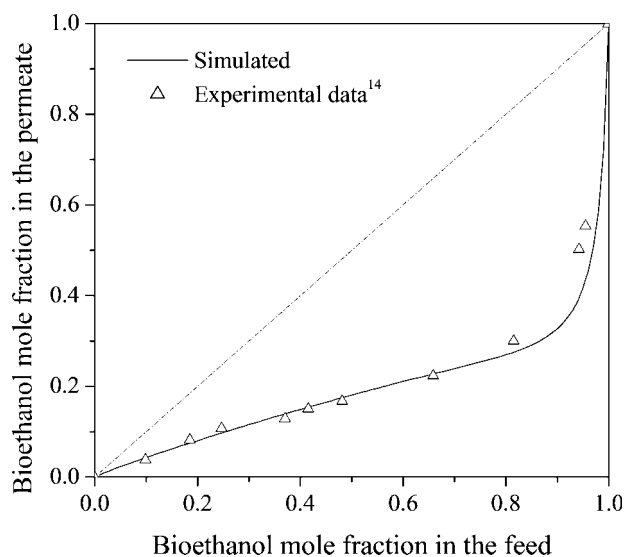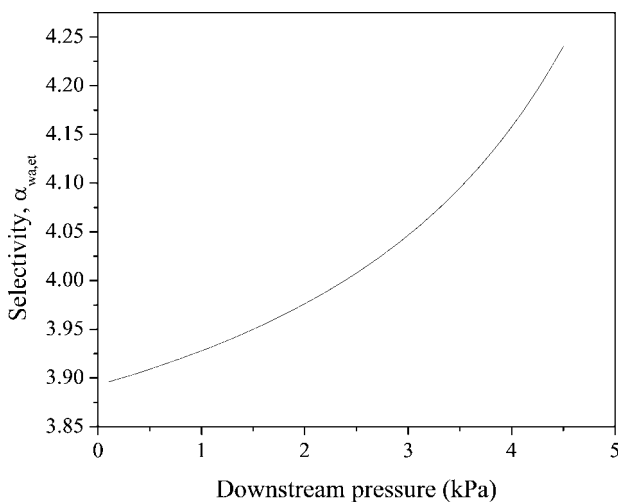

Figure 6 Bioethanol mole fraction in the permeate versus the bioethanol mole fraction in the feed at 310.15 K and 0.133 kPa.
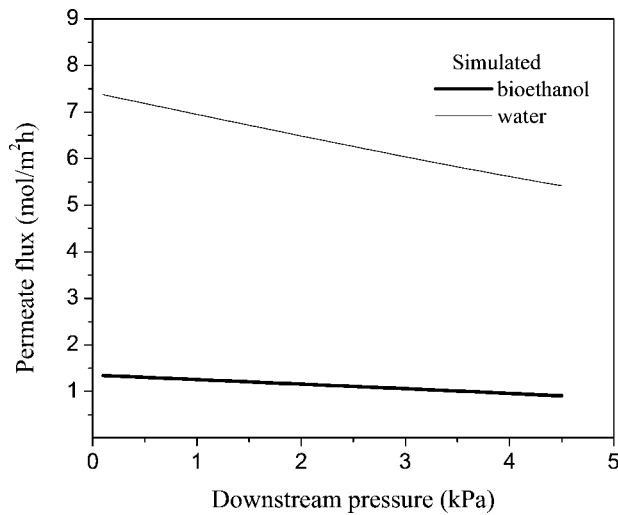
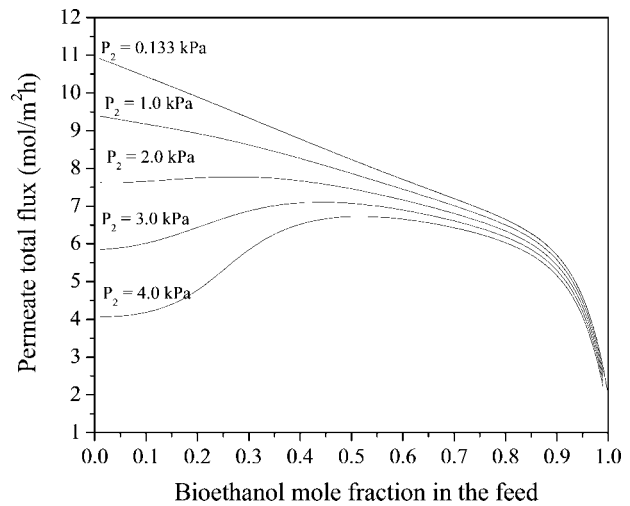**Figure 7** Influence of the pressure on the permeate flux (bioethanol mole fraction of 0.415; 310.15 K).

**Figure 9** Variation of the permeate total flux with the bioethanol composition in the feed at different permeate pressures.

bioethanol/water. It is possible to observe that bioethanol is recovered in the retentate in higher contents than the azeotropic composition. This behavior is presented for different fluxes.

Table IV presents the purity of bioethanol desired in the retentate and its recovery. The retentate flow rate with the required feed flow rate to reach this purity is also presented. It is important to mention that the permeate flux depends on the driving force of the process managed by the reduction of the pressure of the permeate side. Thus, the permeate pressure determines the amount of flux to be permeate.[29] In this case study, the permeate pressure was kept at 0.1 kPa. It was assumed that the permeate flux is constant and independent of the feed flow rate. At 0.1 kPa, the permeate flux is 5.844 mol/m² h ($y_{i,P}$ = 0.317, $y_{j,P}$ = 0.682). The feed was assumed to be

close to the azeotropic point, 89.0% mol of bioethanol and 11.0% mol of water at 101.33 kPa.

The results of Table IV can be better evaluated when plotted as presented in Figure 11. In this illustration, it can be observed that the variation of the desirable purity of bioethanol in the retentate is followed by the variation of the retentate total flow rate and by the recovery. In such way, it can be seen that, maximizing the purity of bioethanol in the retentate stream, the retentate flow rate reduces and, consequently, reduces the recovery.

It is important to emphasize that, in this case study, the pervaporation became possible the separation of the azeotropic mixture bioethanol/water. It was possible to determine the recovery and the purity of bioethanol. Following the methodology

Figure 8 Influence of the pressure on the selectivity (bioethanol mole fraction of 0.415).
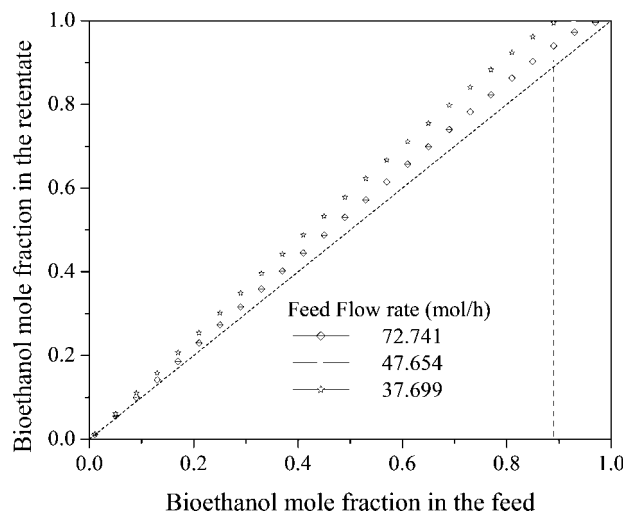
Figure 10 Bioethanol mole fraction in the retentate versus bioethanol mole fraction in the feed at different feed fluxes (310.15 K and 0.133 kPa).
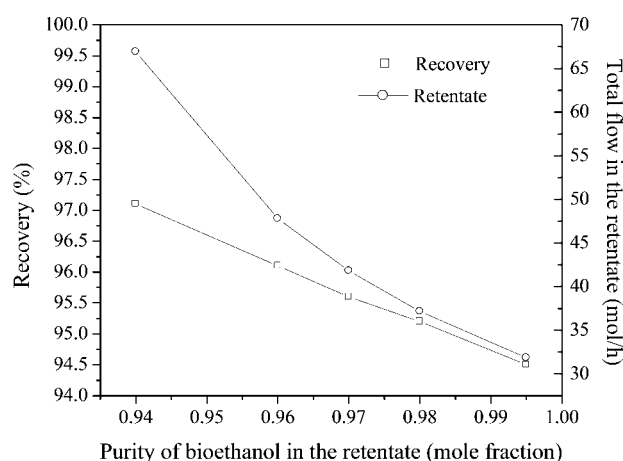
TABLE IV
Recovery and Purity of Bioethanol in the Retentate for Feed Bioethanol Composition of 89.0% mol

Purity of bioethanol in the retentate (% mol)	Feed flow rate (mol/h)	Total retentate flow rate (mol/h)	Recovery of bioethanol in the retentate (%)
94.0	72.7	66.9	97.1
96.0	53.6	47.8	96.1
97.0	47.7	41.8	95.6
98.0	43.0	37.2	95.2
99.5	37.7	31.9	94.5
99.9	36.5	30.7	94.3

applied for the simulations, it is possible to easily evaluate the applicability of this process to other azeotropic mixtures.

CONCLUSIONS

In this work, the separation of bioethanol/water mixtures was studied in PEI membrane, which is highly hydrophilic, indicating that it is useful for the enrichment of bioethanol (retentate). The proposed model is recommended to dense membranes typically used in pervaporation process. Thus, to validate the model, PEI membranes were used, showing good agreement with experimental data, confirming their applicability for separating azeotropic mixtures. The good performance of the model also allows its application for the study of the effect of the process variables, as for example, the downstream pressure and the feed composition on the separation, observing that the increase of bioethanol composition in the feed contributes for the reduction of the water permeation. However, the selectivity increases, proportionally to bioethanol composition, what can be attributed to a higher diffusion of water in the membrane, when low concentration of water is present in the feed. Moreover, it can be verified that it was possible to break the azeotropic point. The developed software, ''PERVAP,'' can also be useful to study other water–organic azeotropic systems.

NOMENCLATURE

Symbols	Definitions
A	membrane area (m^2)
a	activity
C	concentration (mol/m^3)
$D_{i,F}$	diffusion coefficient of component i in the feed stream in eq. (2) (cm^2/s)
D_i^m	diffusion coefficient of component i in the membrane (m^2/h)
D_0	preexponential factor in eq. (25) (cm^2/s)
E	energy required to overcome attractive forces from neighboring molecules (cal/mol)
F	feed flow rate (mol/h)
J	permeate flux (mol/m^2 h)
K_{11}	solvent free-volume parameter (cm^3/gK)
K_{21}	solvent free-volume parameter (K)
K_{22}	polymer free-volume parameter (K)
K_{12}	polymer free-volume parameter (cm^3/gK)
ℓ	membrane thickness (m)
M_j	molecular weight in eq. (2) (g/mol)
p	permeate relative pressure (ratio of downstream pressure and vapor pressure of component i)
P^{sat}	vapor pressure (kPa)
P	pressure (kPa)
Pe	Peclet number
T	temperature (K)
T_{g1}	solvent glass transition temperature (K)
T_{g2}	polymer glass transition temperature (K)
Re	retentate flow rate in eq. (30) (mol/h)
x_{liquid}	mole fraction
y	vapor mole fraction
v	molar partial volume (cm^3/g)
$\widehat{V}_1^*$	specific critical hole free-volume of solvent required for jump (cm^3/g)
$\widehat{V}_2^*$	specific critical hole free-volume of polymer required for jump (cm^3/g)
R	gas constant

Greek letters

γ	overlap factor for free-volume in eq. (25) in the feed phase
$\gamma_{i,F}$, $\gamma_{j,F}$	activity coefficient of components i and j
$\overline{\gamma}_i^m$	activity coefficient in the membrane for component i (m^3/mol)
μ_j	viscosity in eq. (2) (cP)
$\overline{\gamma}_j^m$	activity coefficient in the membrane for component j (m^3/mol)

Figure 11 Influence of the recovery and of the retentate total flow rate on the purity of bioethanol.

μ	chemical potential (J/mol)
μ_0	chemical potential of pure solvent (J/mol)
ω	mass fraction
ξ	ratio of critical molar volume of solvent jumping unit to that of polymer jumping unit
ϕ	volume fraction in eq. (2)
χ	interaction parameter of Flory-Huggins theory
$\Theta_m^{(M)}$	surface area fraction of group m in mixture
α	selectivity
δ_{12}	interaction parameter in eq. (26)
δ_{bl}	boundary layer (m)
ϕ	solvent association parameter in eq. (2)

Subscripts/Superscripts

T	total
F	feed phase
P	permeate phase
i	bioethanol
j	water
m	membrane
1	solvent
2	polymer
R	retentate

References

1. Peng, M.; Vane, L. M.; Liu, S. X. J. Hazard Mater 2003, B98, 69.
2. Pereira, C. C.; Ribeiro, C. P.; Nobrega, R.; Borges, C. P. J Membr Sci 2006, 274, 1.
3. Smitha, B.; Sridhar, S. S.; Ramakrishna, M. J Membr Sci 2004, 241, 1.
4. Ten, P. K.; Field, R. W. Chem Eng Sci 2000, 55, 1425.
5. Marriot, J. I.; Sorense, E.; Bogle, I. D. L. Comp Chem Eng 2001, 25, 693.
6. Brun, J. P.; Larchet, C.; Melet, R.; Bulvestre, G. J Membr Sci 1985, 23, 257.
7. Brun, J. P.; Larchet, C.; Bulvestre, G.; Auclair, B. J Membr Sci 1985, 25, 55.
8. Liu, M. G.; Dickson, J. M.; Côté, P. J Membr Sci 1996, 111, 227.
9. Aminabhavi, T. M.; Naidu, B. V. K.; Sridhar, S.; Rangarajan, R. J Appl Polym Sci 2005, 95, 1143.
10. Hoda, N.; Suggala, S. V.; Bhattacharya, P. K. Comp Chem Eng 2005, 30, 202.
11. Peng, F.; Pan, F.; Li, D.; Jiang, Z. Chem Eng J 2005, 114, 123.
12. Vrentas, J. S.; Duda, J. L. J Polym Sci Part B: Polym Phys 1997, 15, 403.
13. Vrentas, J. S.; Duda, J. L. AIChE J 1979, 25, 1.
14. Huang, R. Y. M.; Feng, X. Sep Sci Technol 1992, 27, 1583.
15. Wilke, C. R.; Chang, P. AIChE J 1955, 1, 264.
16. Gref, R.; Nguyen, Q. T.; Neel, J. Sep Sci Technol 1992, 27, 467.
17. Lee, C. H. J Appl Polym Sci 1975, 19, 83.
18. Kataoka, T.; Tsuru, T.; Nakao, S.; Kimura, S. J Chem Eng Jpn 1991, 24, 326.
19. Lee, B. C.; Danner, R. P. AIChE J 1996, 42, 837.
20. Hong, S. U. Ind Eng Chem Res 1995, 34, 2536.
21. Flory, P. J. Principles of Polymer Chemistry; Cornell University Press: Ithaca, New York, 1953.
22. High, M. S.; Danner, R. P. Fluid Phase Equilib 1989, 53, 323.
23. Fredenslund, A.; Jones, R. L.; Prausnitz, J. M. AIChE J 1975, 21, 1086.
24. Fredenslund, A.; Gmehling, J.; Rasmusen, P. Vapor-Liquid Equilibria Using UNIFAC; Elsevier: Amsterdam, 1977.
25. Neel, J.; Nguyen, Q. T.; Clement, R.; LeBlanc, L. J Membr Sci 1983, 15, 43.
26. Haward, R. N. J Macromol Sci Rev Macromol Chem Phys 1970, 4, 191.
27. Bretas, R. E. S.; Collias, D.; Baird, D. G. Polym Eng Sci 1994, 34, 1492.
28. Chen, F. R.; Chen, H. F. J Membr Sci 1998, 139, 201.
29. Neel, J.; Aptel, P.; Clement, R. Desalination 1985, 53, 297.